Received: 2 May 2022 | Revised: 27 May 2022 | Accepted: 29 May 2022

DOI: 10.1002/mma.8482

RESEARCH ARTICLE

WILEY

Group method analysis for blood-Mn-$ZnFe_2O_4$ flow and heat transfer under ferrohydrodynamics through a stretched cylinder

Jahangir Alam[1] | **Md. Ghulam Murtaza**[2] | **Efstratios Em. Tzirtzilakis**[3] | **Mohammad Ferdows**[1]

[1]Research Group of Fluid Flow Modeling and Simulation, Department of Applied Mathematics, University of Dhaka, Dhaka, Bangladesh

[2]Department of Mathematics, Comilla University, Cumilla, Bangladesh

[3]Fluid Mechanics and Turbomachinary Laboratory, Department of Mechanical Engineering, University of the Peloponnese, Tripoli, Greece

Correspondence
Mohammad Ferdows, Department of Applied Mathematics, University of Dhaka, Dhaka 1000, Bangladesh.
Email: ferdows@du.ac.bd

Communicated by: D. Zeidan

Funding information
National Science and Technology (NST), Bangladesh

In this paper, a steady, viscous, incompressible, and electrically non-conducting laminar flow of biomagnetic fluid, namely, the flow of blood with magnetic particles over a stretched cylinder in the presence of magnetic dipole, is studied. Since magnetic particles with low cytotoxicity can carry away unwanted reactive oxygen species and provide safeguard for biomedical applications, this study has immense applications in medical and bio-engineering sections like cancer treatment, drug delivery, and magnetic resonance imaging (MRI). The problem is first analyzed by applying group theoretical method, namely, one parameter group method. The invariance property of system of partial differential equations (PDEs) under one parameter group method transformations yields the weeny generators. By using the basic theorem of one parameter group method including invariance conditions, the set of PDEs is converted into ordinary differential equations (ODEs), and consequently, the number of independent variables is reduced into one variable. Afterwards, the resulting coupled nonlinear set of ODEs is numerically solved by introducing an efficient numerical technique that based upon common finite difference with central differencing, a tridiagonal matrix manipulation, and finally, an iterative procedure. A comparative graphical analysis of velocity, temperature profiles, skin friction coefficient and rate of heat transfer for blood-Mn-$ZnFe_2O_4$ magnetic fluid has been carried out for various physical parameters such as ferromagnetic interaction parameter and magnetic particles volume fraction etc. The important findings from the present investigation are that the temperature of blood is enhanced for larger values of magnetic particles volume fraction and more effectively than pure blood. It is also found that blood velocity is increased as the ferromagnetic number increases. The skin friction coefficient is enhanced 132.22%, and the rate of heat transfer is increased by 5.86% by the application of magnetic field; whereas for particles volume fraction, skin friction decreases about 0.61%, and rate of heat transfer declines about 4%. Additionally, this study also discloses that the application of group theoretical method is justified in biomagnetic fluid dynamics especially research on blood flow and heat transfer, where the blood flow significantly influenced by the ferromagnetic number. A comparison has been also performed, and the results are found in excellent agreement with previous published in literature. The present study could be considered for magnetic driving of biologically suitable magnetic particles filled with medicine.

KEYWORDS

biomagnetic fluid dynamics (BFD), blood, finite difference method, group theoretical method, magnetic dipole, magnetic particles, stretched cylinder

MSC CLASSIFICATION

76ZXX, 74F10, 92CXX, 76W05

1 | INTRODUCTION

Studies on biological fluid which known as biomagnetic fluid and whose flows are affected in presence of a strong magnetic field are attracted researchers over the last few decades. Because of the fact that all biological fluids contain ion which can interact with a strong applied magnetic field. One of the characteristics of biomagnetic fluid is blood, and it is found that blood act as a diamagnetic material when oxygenated, and when deoxygenated, blood behave as a paramagnetic material. Numerous applications are directly connected in biomedical and bioengineering by considering the studies of biomagnetic fluid dynamics (BFD) particularly in drug and gene delivery as used by magnetic particles, magnetic resonance imaging (MRI) for imaging, reduction of blood during surgeries, in hyperthermia such as cancer treatment, injury treatment, and open heart surgeries as early mentioned by previous works,[1–5] whereas magnetic particles can play a vital role due to their biocompatibility, facile synthesis, and ease that provides abundant functionalized for specific applications.

Biomagnetic fluid dynamics (BFD) is an area in fluid dynamics where the effects of strong magnetic field are analyzed on biological fluid. The first mathematical model of BFD was delivered by Haik et al.[6] In this study, fluid is assumed as isothermal, Newtonian, and electrically non-conducted. After few years back, this model is extended by Tzirtzilakis[7] where both principles of ferrohydrodynamic (FHD) and magnetohydrodynamic (MHD) were considered. The difference between the studies of Haik et al.[6] and Tzirtzilakis[7] is that in Tzirtzilakis,[7] the temperature distribution is studied in the flow field considering non-isothermal field. Second thing is that biological fluid such as blood is considered electrically conducting, and at the same time, polarization forces are also taken into consideration.[7] Numerous studies on 2-D/3-D BFD over stretching/shrinking sheet have been carried out by several researchers in recent past under different circumstances. Murtaza et al.[8] investigated the behavior of biomagnetic fluid considering the magnetic properties such as electrical conductivity along with polarization. In that particular study, they adopted both principles of FHD and MHD and found that BFD formulation has significant positive influence rather than MHD or FHD. While they showed that BFD term remarkably reduced the velocity profile but enhanced the temperature profile comparable to the formulation of MHD or FHD alone. Similar types of attempt were also found in the study of Ferdows et al.[9] which examined the BFD flow in stretched cylindrical surface. The effect of thermal radiation on blood flow and heat transfer through an unsteady stretching sheet with aid principles of FHD and MHD was examined by Alam et al.[10] The effect of magnetic dipole as well as heat source/sink on Maxwell biomagnetic fluid over a three dimensional stretching sheet is investigated by Murtaza et al.[11]

Currently in medical and engineering areas, the study of boundary layer flow and heat transfer of nanofluid took quite interest from researchers. In 1995, Choi[12] was the first who introduced the term nanofluid, where nanoparticles are mixed with the base fluid such as water and oil due to the fact that the enhancement of thermal conductivity of the fluid. Gul et al.[13] examined the mixed convection flow and heat transfer of water based nanofluid over a vertical channel, where both magnetic and non-particles are considered for nanoparticles. In presence of magnetic dipole, Alam et al.[14] examined the biomagnetic fluid flow and heat transfer over a stretching sheet, where blood considered as base fluid and gold considered as nanoparticles. Gholinia et al.[15] studied the influence of magnetic field on $C_2H_6O_2$-Ag and $C_2H_6O_2$-Cu nanofluid through a permeable circular cylinder. While Saranya and Al-Mdallal[16] examined the sodium alginate with three magnetic particles like particles $CoFe_2O_4$, Mn-$ZnFe_2O_4$, and Ni-Fe_2O_4 over an unsteady contracting cylinder under the influence of aligned magnetic field. Mehmood et al.[17] analyzed the effects of hybrid fractional second grade model considering blood as base fluid and Au, Al_2O_3 as nanoparticles through a stenosed aneurysmal artery with heat transfer. Abd Elmabodu et al.[18] presented a mathematical model for unsteady, incompressible, Newtonian peristaltic fluid in a finite length tube with variable viscosity. They observed that the peaks of pressure fluctuate with time and attain various values with non-integral numbers of peristaltic wave. Eldesoky et al.[19] investigated the MHD peristaltic flow that induced motion in a channel over porous medium. A comprehensive study of the peristaltic propulsion of hybrid nanofluid where titanium and gold are considered as nanoparticles under the effects of magnetic field was studied by Bhatti and Abdelsalam.[20] Thumma et al.[21] studied the Maxwell nanofluid under the influence of heat source/sink over a three dimensional stretching sheet. Bhatti et al.[22] evaluated the flow of MHD water based nanofluid, where MgO and Ni are used as nanoparticles over a stretching elastic surface in a porous medium. It is notable that nanoparticle flows are widely investigated considering other engineering applications apart from biomedical. Sheikholeslami et al.[23] examined the influence of novel turbulator on efficiency of solar collector system, where authors considered water as base fluid and MWCNT and Al_2O_3 as hybrid nanoparticles. They found that velocity enhanced about 43.81% for the augment values of revolution. Whereas, Sheikholeslami and Ebrahimpour[24] present an analysis of solar thermal improvement by capitalizing water-based Al_2O_3 nanoparticles. In this paper, authors observed that the heat can increased up to 0.153% as inclusion of nano-powders. Sheikholeslami et al.[25] discussed an hydrothermal analysis of absorber tube with a solar system involving parabolic reflector and found that heat transfer coefficients is enhanced about 180.13% for volume fraction. Sheikholeslami and Ali Farshad[26] inquired the efficacy of nanoparticles over a solar collector invoking helical tapes and saw that nusselt number enhanced about 6.47% for the values of circular gap.

The mathematical assumptions that introduced in this model are applied with the one-parameter group transformation, which further leads to a similarity representation of the given problem. The set of partial differential equations with boundary conditions reduces to a number of independent variables with a systematic formalism. In 1948, Birkhoff[27,28] was the first who introduced the group methods, as a class of methods for reducing the number of independent variables. After that in 1952, Morgan[29] presented a theory that leads to the improvement over the earlier similarity methods and the theory that given by Morgan[29] later on extended by Michal[30] in the same year. To present a general systematic group formalism for similarity analysis, Moran and Gaggioli[31,32] developed an elementary group theory. Abd-el-Malek and Badran[33] studied the steady free convective laminar boundary layer flow on a vertical circular cylinder utilizing the group theoretical analysis. The converted ordinary differential equation with corresponding boundary conditions are those computed numerically by applying fourth-order Runge–Kutta scheme along with a gradient method. El-Kabeir et al.[34] applied the group theoretical transformation to present a mathematical analysis of incompressible, electrically conducting fluid flow and heat transfer over a vertical cone through porous medium under the influence of thermal radiation, where El-Kabeir et al.[35] solved the problem of unsteady MHD combined convection flow over a moving vertical sheet with the group transformation.

Considering the above mentioned studies, the aim of the present study is that to find out the solution of the highly nonlinear BFD problems by means of approaching group theoretical method, namely, one-parameter group transformation. To the authors' best knowledge, such one-parameter group transformations have not been applied to BFD problems where blood take as base fluid and Mn-$ZnFe_2O_4$ considered as magnetic particles over a stretched cylinder under the influence of a magnetic dipole. By applying this method, the number of independent variables is reduced by one, and consequently, the set of PDEs with the boundary conditions is reduced to ODEs with the applicable boundary conditions. Effects of the appearing nondimensional physical parameters such as ferromagnetic interaction parameter, magnetic particles volume fraction, and arbitrary constant for the case of blood-Mn-$ZnFe_2O_4$ on the distribution of velocity, temperature, skin friction coefficient, and rate of heat transfer have been studied and presented graphically.

2 | MATHEMATICAL FORMULATION WITH GOVERNING EQUATIONS

An incompressible, viscous, two-dimensional steady laminar boundary layer flow of biomagnetic fluid, namely, the flow of blood with magnetic particles (Mn-$ZnFe_2O_4$) through a stretched cylinder, is considered in this study, where cylinder is stretched with velocity $u_w{}^* = \frac{u_0 z^*}{L}$, u_0 is referred velocity, and L is the characteristic length of the cylinder. Also it is considered that the radius of the cylinder is R^*, the axis z^* is taken along the flow, and r^* axis is normal to the cylinder as shown in Figure 1. We also assumed that the surface temperature and ambient fluid temperature that situated far away from the surface are T_w and T_c, respectively, with $T_w < T_c$. A magnetic dipole creates a magnetic field of strength that locates below from the sheet with considering the distance c. Under the above assumptions, the idea of

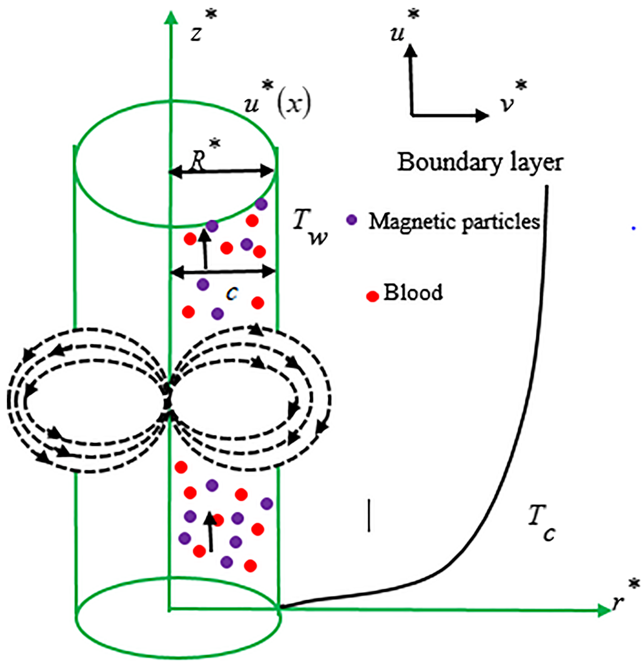

FIGURE 1 Physical model and coordinate system [Colour figure can be viewed at wileyonlinelibrary.com]

Abd-el-Malek and Badran[33] is explored, and therefore, the governing equations in cylindrical coordinates can be written as

$$\frac{\partial u^*}{\partial z^*}+\frac{v^*}{r^*}+\frac{\partial v^*}{\partial r^*}=0 \tag{1}$$

$$u^*\frac{\partial u^*}{\partial z^*}+v^*\frac{\partial u^*}{\partial r^*}=\frac{\mu_{mf}}{\rho_{mf}}\left(\frac{1}{r^*}\frac{\partial u^*}{\partial r^*}+\frac{\partial^2 u^*}{\partial r^{*2}}\right)+\frac{1}{\rho_{mf}}\mu_0 M\frac{\partial H^*}{\partial z^*} \tag{2}$$

$$(\rho C_p)_{mf}\left(u^*\frac{\partial T^*}{\partial z^*}+v^*\frac{\partial T^*}{\partial r^*}\right)+\mu_0\, T^*\frac{\partial M}{\partial T^*}\left(u^*\frac{\partial H^*}{\partial z^*}+v^*\frac{\partial H^*}{\partial r^*}\right)=\kappa_{mf}\left(\frac{1}{r^*}\frac{\partial T^*}{\partial r^*}+\frac{\partial^2 T^*}{\partial r^{*2}}\right) \tag{3}$$

with associated boundary conditions:

$$u^*=0\,,\ v^*=0\,,\ T^*=T_w \qquad \text{at } r^*=R^* \tag{4}$$

$$u^*\to 0\,,\ T^*\to T_c \qquad \text{as } r^*\to\infty \tag{5}$$

Here, u^* and v^* are the dimensional velocity components along z^* and r^* directions. μ_0 is the magnetic permeability, H^* is the magnetic field of strength intensity, and M is the magnetization. Furthermore, κ, ρ, C_p, μ are known as bio-magnetic fluid thermal conductivity, density, specific heat at constant pressure, and dynamic viscosity, respectively, where the subscript symbols $(\ )_{mf}$ mean magnetic fluid. The magnetic force arises due to the polarization, and mathematically, this term is represented by $\mu_0 M\frac{\partial H^*}{\partial z^*}$ while the term $\mu_0\ T^*\frac{\partial M}{\partial T^*}\left(u^*\frac{\partial H^*}{\partial z^*}+v^*\frac{\partial H^*}{\partial r^*}\right)$ in Equation (3) indicates thermal conductivity per unit volume, and these two terms are commonly known in FHD.

Following the studies,[36,37] a magnetic dipole produces a magnetic field $\overrightarrow{H^*}=(H_z{}^*, H_r{}^*)$ whose components H_z^* and H_r^* are given by the following.

$$H_z^*\ (z^*, r^*) = \frac{\gamma}{2\pi} \frac{z^{*2} - (r^* + c)^2}{\left(z^{*2} + (r^* + c)^2\right)^2} \tag{6}$$

$$H_r^*\ (z^*, r^*) = \frac{\gamma}{2\pi} \frac{2z^*\ (r^* + c)}{\left(z^{*2} + (r^* + c)^2\right)^2} \tag{7}$$

According to Nadeem et al. and Tahir et al.,[36,37] the analogous manipulations of the Equations (6) and (7) take the following form:

$$\frac{\partial H^*}{\partial z^*} = -\frac{\gamma}{2\pi} \frac{2z^*}{(r^* + c)^4} \tag{8}$$

$$\frac{\partial H^*}{\partial r^*} = -\frac{\gamma}{2\pi} \left(\frac{-2}{(r^* + c)^3} + \frac{4z^{*2}}{(r^* + c)^5} \right) \tag{9}$$

Thus, the magnetic field of intensity H^* can be expressed as follows.

$$H^*(z^*, r^*) = \frac{\gamma}{2\pi} \left(\frac{1}{(r^* + c)^2} - \frac{z^{*2}}{(r^* + c)^4} \right) \tag{10}$$

Again the relation between magnetization M of the biomagnetic fluid with temperature T^* and the magnetic field intensity H^* can be defined in the following way as suggested by[38]

$$M = KH^*(T_c - T^*) \tag{11}$$

where K is the pyromagnetic coefficient and T_c is the Curie temperature.

The characteristics of magnetic fluids are expressed as follows[39]:

$$\mu_{mf} = \mu_f\ (1-\varphi)^{-2.5},\ (\rho C_p)_{mf} = (1-\varphi)(\rho C_p)_f + \varphi\ (\rho C_p)_s\ ,\ \rho_{mf} = (1-\varphi)\rho_f + \varphi\rho\ _s,\ \frac{\kappa_{mf}}{\kappa_f} = \frac{(\kappa_s + 2\ \kappa_f) - 2\ \varphi\ (\kappa_f - \kappa_s)}{(\kappa_s + 2\kappa_f) + \varphi\ (\kappa_f - \kappa_s)} \tag{12}$$

Here, the subscript symbols $()_f$ and $()_s$ indicate base fluid (blood) and magnetic particles (Mn-ZnFe_2O_4).

Next step is to introduce the nondimensional boundary layer variables, and it takes the following form:

$$z = \frac{z^*}{R^*}, r = \frac{r^*}{R^*}, u = \frac{u^* R^*}{\upsilon_f}, v = \frac{v^* R^*}{\upsilon_f}, H = \frac{H^*}{H_0}, \theta = \frac{T_c - T^*}{T_c - T_w} \tag{13}$$

Using (13) and definitions of (12), Equations (1)–(3) along with boundary conditions (4) and (5) are taking the following dimensionless form:

$$\frac{\partial u}{\partial z} + \frac{v}{r} + \frac{\partial v}{\partial r} = 0 \tag{14}$$

$$(1-\varphi)^{2.5} \left(1 - \varphi + \varphi \frac{\rho_s}{\rho_f} \right) \left(u \frac{\partial u}{\partial z} + v \frac{\partial u}{\partial r} \right) = \frac{1}{r} \frac{\partial u}{\partial r} + \frac{\partial^2 u}{\partial r^2} + (1-\varphi)^{2.5} \beta H \theta \frac{\partial H}{\partial z} \tag{15}$$

$$\frac{\kappa_f}{\kappa_{mf}}\left(1-\varphi+\varphi\frac{(\rho C_p)_s}{(\rho C_p)_f}\right)\Pr\left(u\frac{\partial\theta}{\partial z}+v\frac{\partial\theta}{\partial r}\right)+\frac{\kappa_f}{\kappa_{mf}}\beta\ EcH(\varepsilon-\theta)\left(u\frac{\partial H}{\partial z}+v\frac{\partial H}{\partial r}\right)=\frac{1}{r}\frac{\partial\theta}{\partial r}+\frac{\partial^2\theta}{\partial r^2} \tag{16}$$

Along with corresponding boundary conditions

$$u=0\ ,\ v=0\ ,\ \theta=1\,\text{at}\,r=1 \tag{17}$$

$$u\to0\ ,\ \theta\to0\,\text{as}\,r\to\infty \tag{18}$$

where ferromagnetic interaction parameter $\beta=\frac{\mu_0KH_0^2(T_c-T_w)R^{*2}\rho_f}{\mu_f^2}$; Eckert number $Ec=\frac{\mu_f^3}{R^{*2}k_f\ (T_c-T_w)\rho_f^2}$; Curie temperature $\varepsilon=\frac{T_c}{T_c-T_w}$; Prandtl number $\Pr=\frac{(\mu C_p)_f}{\kappa_f}$.

Now we set $ru=\frac{\partial\psi}{\partial r}$ and $rv=-\frac{\partial\psi}{\partial z}$, and therefore, Equations (15) and (16) become as follows:

$$(1-\varphi)^{2.5}\left(1-\varphi+\varphi\frac{\rho_s}{\rho_f}\right)\left[r\frac{\partial\psi}{\partial r}\frac{\partial^2\psi}{\partial z\partial r}+\frac{\partial\psi}{\partial z}\left(\frac{\partial\psi}{\partial r}-r\frac{\partial^2\psi}{\partial r^2}\right)\right]=\frac{\partial\psi}{\partial r}-r\frac{\partial^2\psi}{\partial r^2}+r^2\frac{\partial^3\psi}{\partial r^3}+(1-\varphi)^{2.5}\beta Hr^3\theta\frac{\partial H}{\partial z} \tag{19}$$

$$\frac{\kappa_f}{\kappa_{mf}}\left(1-\varphi+\varphi\frac{(\rho C_p)_s}{(\rho C_p)_f}\right)\Pr\left(\frac{\partial\psi}{\partial r}\frac{\partial\theta}{\partial z}-\frac{\partial\psi}{\partial z}\frac{\partial\theta}{\partial r}\right)+\frac{\kappa_f}{\kappa_{mf}}\beta\ EcH(\varepsilon-\theta)\left(\frac{\partial\psi}{\partial r}\frac{\partial H}{\partial z}-\frac{\partial\psi}{\partial z}\frac{\partial H}{\partial r}\right)=\frac{\partial\theta}{\partial r}+r\frac{\partial^2\theta}{\partial r^2} \tag{20}$$

The boundary conditions (17) and (18) are reduced as follows:

$$\frac{\partial\psi}{\partial r}=0\ ,\ \frac{\partial\psi}{\partial z}=0\ ,\ \theta=1\ \text{at}\ r=1 \tag{21}$$

$$\frac{\partial\psi}{\partial r}\to0\ ,\ \theta\to0\ \text{as}\ r\to\infty \tag{22}$$

3 | SOLUTION OF THE PROBLEM USING GROUP FORMULATION

The partial differential Equations (19)–(22) are now solved by applying a one-parameter group transformation following the studies of Moran and Gaggioli and El-Kabeir et al.[32,34] For this, we initially need to subgroup the transformations. Afterwards, the number of independent variables will be reduced by one variable, and the governing partial differential Equations (19)–(21) are converted into a system of ordinary differential equations containing only one-parameter variable in terms of similarity variable.

3.1 | The group systematic formulation

The procedure is initiated with the group G, a class of one parameter "a" of the form

$$G:\begin{cases}\bar{z}=C^z(a)z+k^z(a)\\ \bar{r}=C^r(a)r+k^r(a)\\ \bar{\psi}=C^\psi(a)\psi+k^\psi(a)\\ \bar{\theta}=C^\theta(a)\theta+k^\theta(a)\\ \bar{H}=C^H(a)H+k^H(a)\end{cases} \tag{23}$$

where C^s and k^s are real-value functions and at least differentiable in their real argument "a."

3.2 | The invariance analysis

To transform the differential equations, transformations of the derivatives are obtained from G via chain-rule operations:

$$\begin{aligned} \frac{\partial \overline{S}}{\partial \overline{i}} &= \frac{C^s}{C^i}\frac{\partial S}{\partial i} \\ \frac{\partial^2 \overline{S}}{\partial \overline{i}^2} &= \frac{C^s}{\left(C^i\right)^2}\frac{\partial S}{\partial i^2} \end{aligned} \tag{24}$$

where S stands for ψ,θ,H and $i=z,r$.

Equation (19) is said to be invariantly transformed whenever

$$\begin{aligned} &(1-\varphi)^{2.5}\left(1-\varphi+\varphi\frac{\rho_s}{\rho_f}\right)\left[\overline{r}\frac{\partial\overline{\psi}}{\partial\overline{r}}\frac{\partial^2\overline{\psi}}{\partial\overline{z}\partial\overline{r}}+\frac{\partial\overline{\psi}}{\partial\overline{z}}\left(\frac{\partial\overline{\psi}}{\partial\overline{r}}-\overline{r}\frac{\partial^2\overline{\psi}}{\partial\overline{r}^2}\right)\right]-\frac{\partial\overline{\psi}}{\partial\overline{r}}+\overline{r}\frac{\partial^2\overline{\psi}}{\partial\overline{r}^2}-\overline{r}^2\frac{\partial^3\overline{\psi}}{\partial\overline{r}^3} \\ &-(1-\varphi)^{2.5}\beta\overline{H}\overline{r}^3\overline{\theta}\frac{\partial\overline{H}}{\partial\overline{r}}=H_1(a)\left[\begin{array}{l}(1-\varphi)^{2.5}\left(1-\varphi+\varphi\frac{\rho_s}{\rho_f}\right)\left[r\frac{\partial\psi}{\partial r}\frac{\partial^2\psi}{\partial z\partial r}+\frac{\partial\psi}{\partial z}\left(\frac{\partial\psi}{\partial r}-r\frac{\partial^2\psi}{\partial r^2}\right)\right] \\ -\frac{\partial\psi}{\partial r}+r\frac{\partial^2\psi}{\partial r^2}-r^2\frac{\partial^3\psi}{\partial r^3}-(1-\varphi)^{2.5}\beta H r^3\theta\frac{\partial H}{\partial z}\end{array}\right] \end{aligned} \tag{25}$$

where $H_1(a)$ is an arbitrary function of the one group parameter "a" which may be constant.

Now Equation (25) yields,

$$\begin{aligned} &(1-\varphi)^{2.5}\left(1-\varphi+\varphi\frac{\rho_s}{\rho_f}\right)\left[\frac{(C^\psi)^2}{C^zC^r}r\frac{\partial\psi}{\partial r}\frac{\partial^2\psi}{\partial z\partial r}+\frac{(C^\psi)^2}{C^zC^r}\frac{\partial\psi}{\partial z}\left(\frac{\partial\psi}{\partial r}-r\frac{\partial^2\psi}{\partial r^2}\right)\right] \\ &-\frac{C^\psi}{C^r}\frac{\partial\psi}{\partial r}+\frac{C^\psi}{C^r}r\frac{\partial^2\psi}{\partial r^2}-\frac{C^\psi}{C^r}r^2\frac{\partial^3\psi}{\partial r^3}-\frac{\left(C^r\right)^3C^\theta\left(C^H\right)^2}{C^z}(1-\varphi)^{2.5}\beta H r^3\theta\frac{\partial H}{\partial z}+R_1 \\ &=H_1(a)\left[\begin{array}{l}(1-\varphi)^{2.5}\left(1-\varphi+\varphi\frac{\rho_s}{\rho_f}\right)\left[r\frac{\partial\psi}{\partial r}\frac{\partial^2\psi}{\partial z\partial r}+\frac{\partial\psi}{\partial z}\left(\frac{\partial\psi}{\partial r}-r\frac{\partial^2\psi}{\partial r^2}\right)\right] \\ -\frac{\partial\psi}{\partial r}+r\frac{\partial^2\psi}{\partial r^2}-r^2\frac{\partial^3\psi}{\partial r^3}-(1-\varphi)^{2.5}\beta H r^3\theta\frac{\partial H}{\partial z}\end{array}\right] \end{aligned} \tag{26}$$

where

$$\begin{aligned} R_1=&(1-\varphi)^{2.5}\left(1-\varphi+\varphi\frac{\rho_s}{\rho_f}\right)\frac{(C^\psi)^2k^r}{C^z(C^r)^2}\left[\frac{\partial\psi}{\partial r}\frac{\partial^2\psi}{\partial z\partial r}-\frac{\partial\psi}{\partial z}\frac{\partial^2\psi}{\partial r^2}\right]+\frac{C^\psi k^r}{(C^r)^2}\frac{\partial^2\psi}{\partial r^2}-\frac{C^\psi k^r}{(C^r)^3} \\ &\times(2rC^r+k^r)\frac{\partial^3\psi}{\partial r^3}-\frac{\left(C^r\right)^3C^\theta\left(C^H\right)k^H}{C^z}(1-\varphi)^{2.5}\beta\, r^3\theta-\frac{\left(C^r\right)^3\left(C^H\right)^2k^\theta}{C^z}(1-\varphi)^{2.5} \\ &\times\beta\, r^3\frac{\partial H}{\partial z}\left(H+k^H\right)-\left[3(C^rr)^2k^r+3rC^r(k^r)^2+(k^r)^3\right]\left[\frac{\left(C^H\right)^2C^\theta}{C^z}(1-\varphi)^{2.5}\beta\, H\theta\frac{\partial H}{\partial z}\right. \\ &\left.+\frac{\left(C^H\right)C^\theta}{C^z}(1-\varphi)^{2.5}\beta\,\theta\frac{\partial H}{\partial z}+\frac{\left(C^H\right)k^\theta}{C^z}(1-\varphi)^{2.5}\beta\, H\theta\frac{\partial H}{\partial z}\left(C^H+1\right)\right] \end{aligned} \tag{27}$$

For invariant transformation, R_1 is equated to zero and this satisfied by setting the following.

$$k^r = k^H = k^\theta = 0 \tag{28}$$

And comparing the coefficients of Equation (26) on both sides and with $H_1(a)$, we get,

$$H_1(a) = \frac{(C^\psi)^2}{C^z C^r} = \frac{(C^r)^3 C^\theta (C^H)^2}{C^z} = \frac{C^\psi}{C^r} \tag{29}$$

where $H_1(a)$ = constant.

In similar way, Equation (20) is said to be invariantly transformed, whenever there is a function $H_2(a)$ such that

$$\begin{aligned}
&\frac{\kappa_f}{\kappa_{mf}}\left(1-\varphi+\varphi\frac{(\rho C_p)_s}{(\rho C_p)_f}\right)\Pr\left(\frac{\partial\overline{\psi}}{\partial\overline{r}}\frac{\partial\overline{\theta}}{\partial\overline{z}}-\frac{\partial\overline{\psi}}{\partial\overline{z}}\frac{\partial\overline{\theta}}{\partial\overline{r}}\right)+\frac{\kappa_f}{\kappa_{mf}}\beta Ec\overline{H}\varepsilon\left(\frac{\partial\overline{\psi}}{\partial\overline{r}}\frac{\partial\overline{H}}{\partial\overline{z}}-\frac{\partial\overline{\psi}}{\partial\overline{z}}\frac{\partial\overline{H}}{\partial\overline{r}}\right)\\
&-\frac{\kappa_f}{\kappa_{mf}}\beta\ Ec\overline{H\theta}\left(\frac{\partial\overline{\psi}}{\partial\overline{r}}\frac{\partial\overline{H}}{\partial\overline{z}}-\frac{\partial\overline{\psi}}{\partial\overline{z}}\frac{\partial\overline{H}}{\partial\overline{r}}\right)-\left(\frac{\partial\overline{\theta}}{\partial\overline{r}}+\overline{r}\frac{\partial^2\overline{\theta}}{\partial\overline{r}^2}\right)\\
&=H_2(a)\left[\begin{aligned}&\frac{\kappa_f}{\kappa_{mf}}\left(1-\varphi+\varphi\frac{(\rho C_p)_s}{(\rho C_p)_f}\right)\Pr\left(\frac{\partial\psi}{\partial r}\frac{\partial\theta}{\partial z}-\frac{\partial\psi}{\partial z}\frac{\partial\theta}{\partial r}\right)+\frac{\kappa_f}{\kappa_{mf}}\beta\ EcH\varepsilon\left(\frac{\partial\psi}{\partial r}\frac{\partial H}{\partial z}-\frac{\partial\psi}{\partial z}\frac{\partial H}{\partial r}\right)\\&-\frac{\kappa_f}{\kappa_{mf}}\beta\ EcH\theta\left(\frac{\partial\psi}{\partial r}\frac{\partial H}{\partial z}-\frac{\partial\psi}{\partial z}\frac{\partial H}{\partial r}\right)-\left(\frac{\partial\theta}{\partial r}+r\frac{\partial^2\theta}{\partial r^2}\right)\end{aligned}\right]
\end{aligned}\tag{30}$$

and Equation (30) reduces to

$$\begin{aligned}
&\frac{\kappa_f}{\kappa_{mf}}\left(1-\varphi+\varphi\frac{(\rho C_p)_s}{(\rho C_p)_f}\right)\Pr\frac{C^\psi C^\theta}{C^r C^z}\left(\frac{\partial\psi}{\partial r}\frac{\partial\theta}{\partial z}-\frac{\partial\psi}{\partial z}\frac{\partial\theta}{\partial r}\right)\\
&+\frac{\kappa_f}{\kappa_{mf}}\frac{(C^\psi)^2(C^H)^2}{C^r C^z}\beta EcH\varepsilon\left(\frac{\partial\psi}{\partial r}\frac{\partial H}{\partial z}-\frac{\partial\psi}{\partial z}\frac{\partial H}{\partial r}\right)\\
&-\frac{\kappa_f}{\kappa_{mf}}\frac{C^\psi C^\theta(C^H)^2}{C^r C^z}\beta\ EcH\theta\left(\frac{\partial\psi}{\partial r}\frac{\partial H}{\partial z}-\frac{\partial\psi}{\partial z}\frac{\partial H}{\partial r}\right)-\frac{C^\theta}{C^r}\left(\frac{\partial\theta}{\partial r}+r\frac{\partial^2\theta}{\partial r^2}\right)+R_2\\
&=H_2(a)\left[\begin{aligned}&\frac{\kappa_f}{\kappa_{mf}}\left(1-\varphi+\varphi\frac{(\rho C_p)_s}{(\rho C_p)_f}\right)\Pr\left(\frac{\partial\psi}{\partial r}\frac{\partial\theta}{\partial z}-\frac{\partial\psi}{\partial z}\frac{\partial\theta}{\partial r}\right)+\frac{\kappa_f}{\kappa_{mf}}\beta\ EcH\varepsilon\left(\frac{\partial\psi}{\partial r}\frac{\partial H}{\partial z}-\frac{\partial\psi}{\partial z}\frac{\partial H}{\partial r}\right)\\&-\frac{\kappa_f}{\kappa_{mf}}\beta\ EcH\theta\left(\frac{\partial\psi}{\partial r}\frac{\partial H}{\partial z}-\frac{\partial\psi}{\partial z}\frac{\partial H}{\partial r}\right)-\left(\frac{\partial\theta}{\partial r}+r\frac{\partial^2\theta}{\partial r^2}\right)\end{aligned}\right]
\end{aligned}\tag{31}$$

where

$$\begin{aligned}
R_2=&\frac{\kappa_f}{\kappa_{mf}}\frac{C^\psi C^H k^H}{C^r C^z}\beta\ Ec\varepsilon\left(\frac{\partial\psi}{\partial r}\frac{\partial H}{\partial z}-\frac{\partial\psi}{\partial z}\frac{\partial H}{\partial r}\right)\\
&-\frac{\kappa_f}{\kappa_{mf}}\frac{C^\psi C^\theta(C^H)^2}{C^r C^z}\beta\ Ec\left[\frac{C^\psi k^\theta(C^H)^2}{C^r C^z}+\frac{C^\psi C^\theta C^H k^H}{C^z}\theta+\frac{C^\psi C^H k^\theta k^H}{C^z C^r}\right]\\
&\times\left(\frac{\partial\psi}{\partial r}\frac{\partial H}{\partial z}-\frac{\partial\psi}{\partial z}\frac{\partial H}{\partial r}\right)-\frac{C^\theta k^r}{(C^r)^2}\frac{\partial^2\theta}{\partial r^2}
\end{aligned}\tag{32}$$

Again for the transformation of invariant, R_2 is equal to zero if the following setting is satisfied

$$k^r = k^H = k^\theta = 0 \tag{33}$$

and

$$H_2(a) = \frac{C^\psi C^\theta}{C^z C^r} = \frac{C^\psi C^\theta \left(C^H\right)^2}{C^z C^r} = \frac{C^\psi \left(C^H\right)^2}{C^z C^r} = \frac{C^\theta}{C^r} \tag{34}$$

where $H_2(a) = \text{constant}$.

The invariance of the boundary conditions (21) and (22) under transformations of (23) and (24) implies

$$C^r = 1 \text{ and } C^\theta = 1 \tag{35}$$

In addition of those conditions given by Equation (28).

Now combining Equations (29) and (34) and invoking (28), (33), and (35), we have the following.

$$C^\psi = C^H = C^z \tag{36}$$

Finally, we get the invariantly transformations of (19)–(22) in one parameter group G. Substitute the values of (28), (33), (35), and (36) in (23), and the group G takes the following form:

$$G: \begin{cases} \bar{z} = C^z(a)z + k^z(a) \\ \bar{r} = r \\ \bar{\psi} = C^z(a)\psi + k^\psi(a) \\ \bar{\theta} = \theta \\ \bar{H} = C^z(a)H \end{cases} \tag{37}$$

3.3 | The complete set of invariants

Our ultimate purpose is of use the group methods in order to represent the given problem in the form of an ordinary differential equation (similarity representation) in a single independent variable (similarity variable). Then we have to proceed in our present analysis to get a complete set of absolute invariants. The complete set of invariants is as follows:

i. The absolute invariants of the independent variables (z, r) are $\eta = \eta\,(z, r)$.
ii. The absolute invariants of the dependent variables (ψ, H, θ)

$$g_j\,(z, r, \psi, H, \theta) = F_j(\eta(z, r)) \qquad , j = 1,\ 2,\ 3.$$

The application of a basic theorem of group theory as stated by Morgan and Moran and Gaggioli[29,32] and states that a function $g_j\,(z, r, \psi, H, \theta)$ is an absolute invariant of a one-parameter group if it satisfies the following first-order linear differential equation:

$$\sum_{i=1}^{5} (\alpha_i S_i + \beta_i) \frac{\partial g}{\partial S_i} = 0 \tag{38}$$

where

$$\begin{aligned} S_i &= z, r, \psi, H, \theta \\ \alpha_i &= \frac{\partial C^s}{\partial a}(a^0) \\ \beta_i &= \frac{\partial k^s}{\partial a}(a^0) \qquad\qquad i = 1,\ 2,\ 3,\ 4,\ 5 \end{aligned} \tag{39}$$

Such that,

$$\begin{aligned} \alpha_1 &= \frac{\partial C^z}{\partial a}(a^0),\ \alpha_2 = \frac{\partial C^r}{\partial a}(a^0),\ \alpha_3 = \frac{\partial C^\psi}{\partial a}(a^0),\ \alpha_4 = \frac{\partial C^H}{\partial a}(a^0),\ \alpha_5 = \frac{\partial C^\theta}{\partial a}(a^0) \\ \beta_1 &= \frac{\partial k^z}{\partial a}(a^0),\ \beta_2 = \frac{\partial k^r}{\partial a}(a^0),\ \beta_3 = \frac{\partial k^\psi}{\partial a}(a^0),\ \beta_4 = \frac{\partial k^H}{\partial a}(a^0),\ \beta_5 = \frac{\partial k^\theta}{\partial a}(a^0) \end{aligned}$$

where a^0 denotes the value of "a" which yields the identity element of the group G.

3.3.1 | Absolute invariants of independent variables

Since $k^r = k^H = k^\theta = 0$ and $C^r = C^\theta = 1$; which gives $\alpha_2 = \alpha_5 = \beta_2 = \beta_4 = \beta_5 = 0$. Now the absolute invariant $\eta(z, r)$ of the independent variables (z, r) is obtained by using Equation (38) when it satisfy the first-order differential equation:

$$(\alpha_1 z + \beta_1)\frac{\partial \eta}{\partial z} + (\alpha_2 r + \beta_2)\frac{\partial \eta}{\partial r} = 0 \tag{40}$$

So the solution of (40) is given by the following.

$$\eta = \eta\ (r) \tag{41}$$

3.3.2 | Absolute invariants of the dependent variables

Now the next step is to find out the absolute invariants of dependent variables. Since from Equation (37) we see that θ is itself an absolute invariant, thus, we have the following.

$$g\ (z, r; \theta) = \theta(\eta) \tag{42}$$

Following the similar manner of (40), we also get the absolute invariants of dependent variables which takes the following form:

$$\begin{aligned} \psi\ (z, r) &= \phi(z) F(\eta) \\ H(z, r) &= \omega(z) E(\eta) \end{aligned} \tag{43}$$

where $\phi(z), \omega(z), F(\eta), E(\eta)$ are functions to be determined. Since $H(z, r), \omega(z)$ are independent of r whereas η depends on r, it follows that $E(\eta)$ must be equal to a constant say E_0. Thus, Equation ((43) becomes the following.

$$\begin{aligned} \psi\ (z, r) &= \phi(z) F(\eta) \\ H(z, r) &= \omega(z) E_0 \end{aligned} \tag{44}$$

The functions of $\phi(z),\omega(z)$ will be determined later on, like that the set of governing Equations (2) and (3) is transformed into a set of ordinary differential equations of functions $F(\eta),\theta(\eta)$.

3.4 | The reduction to an ordinary differential equation

Now the set of ordinary differential equations is obtained by using the forms of establishment of dependent and independent absolute invariant as we early discussed where the absolute invariant of independent may assumed in the following form:

$$\eta = r \tag{45}$$

Using the above transformations of (44) and (45), we get the following set of ordinary differential equation:

$$\begin{aligned} r^2F''' &+ \left[(1-\varphi)^{2.5}\left(1-\varphi+\varphi\frac{\rho_s}{\rho_f}\right)k_1F-1\right]rF'' \\ &+\left[1-(1-\varphi)^{2.5}\left(1-\varphi+\varphi\frac{\rho_s}{\rho_f}\right)\left(rk_1F'+k_1F\right)\right]F'+(1-\varphi)^{2.5}k_2r^3\beta\theta=0 \end{aligned} \tag{46}$$

$$r\theta''+\left[1+\left(1-\varphi+\varphi\frac{(\rho C_p)_s}{(\rho C_p)_f}\right)\frac{\kappa_f}{\kappa_{mf}}k_1\mathrm{Pr}F\right]\theta'-\frac{\kappa_f}{\kappa_{mf}}k_3\beta\ Ec\ (\varepsilon-\theta)F''=0 \tag{47}$$

With applicable boundary conditions,

$$F=F'=0\ ,\ \theta=1\ \text{ at } r=1 \tag{48}$$

$$F'\to 0\ ,\ \theta\to 0\ \text{ as } r\to\infty \tag{49}$$

where the arbitrary coefficients are determined by the following expression:

$$k_1=\frac{\partial\phi}{\partial z},\ k_2=\frac{\omega}{\phi}E_0^2\frac{\partial\omega}{\partial z},k_3=\phi\omega E_0^2\frac{\partial\omega}{\partial z} \tag{50}$$

Case 1: Consider $k_2=k_3=1$. Equations (46) and (47) yield

$$\begin{aligned} r^2F''' &+ \left[(1-\varphi)^{2.5}\left(1-\varphi+\varphi\frac{\rho_s}{\rho_f}\right)k_1F-1\right]rF'' \\ &+\left[1-(1-\varphi)^{2.5}\left(1-\varphi+\varphi\frac{\rho_s}{\rho_f}\right)\left(rk_1F'+k_1F\right)\right]F'+(1-\varphi)^{2.5}r^3\beta\theta=0 \end{aligned} \tag{51}$$

$$r\theta''+\left[1+\left(1-\varphi+\varphi\frac{(\rho C_p)_s}{(\rho C_p)_f}\right)\frac{\kappa_f}{\kappa_{mf}}k_1\mathrm{Pr}F\right]\theta'-\frac{\kappa_f}{\kappa_{mf}}\beta\ Ec\ (\varepsilon-\theta)F''=0 \tag{52}$$

with corresponding boundary conditions.

$$F=F'=0\ ,\ \theta=1\ \text{ at } r=1 \tag{53}$$

$$F' \to 0\ ,\ \theta \to 0\ \text{ as } r \to \infty \tag{54}$$

The similar attempt is already discussed by [33] when the values $\beta = 1,\ \varphi = Ec = 0$ is considered for (51) and (52).

Moreover, the characteristics of velocity components in boundary layer are as follows:

i. The vertical velocity component $u = \frac{1}{r}(k_1 z + C_1)F'$; C_1 is an integrating constant.
ii. The radial velocity component $v = \frac{k_1}{r}F$.

4 | NUMERICAL PROCEDURE

Now the set of ordinary differential Equations (51) and (52) with corresponding boundary conditions (53) and (54) are solved by using an efficient numerical technique; see Kafoussias and Williams.[40] This numerical technique has better stability characteristics and is simple and efficient. The main things of this technique are that it is constituted with the following features:

1. It is based on the common finite difference method with central differencing.
2. On a tridiagonal matrix manipulation, and
3. On an iterative procedure.

The important part of this numerical technique is to set up a finite effective value of η_∞, convergence criteria ε_1, and step size h. In whole numerical calculations, we assume $h = \Delta\eta = 0.01$, $\varepsilon_1 = 10^{-3}$, and $\eta_\infty = 1$. The numerical procedure continues until the desired accuracy is obtained. For ensuring the accuracy of numerical technique, it is needed to check the present values with earlier documented. For that, we compare our results with Abd-el-Malek and Badran[33] in terms of velocity and temperature profiles, and the results are found in excellent agreement and presented by Figures 2 and 3.

5 | ESTIMATION OF VALUES OF PHYSICAL PARAMETERS

Since our present model is known as biomagnetic fluid model (BFD), where blood take as base fluid and manganese franklinite ($Mn\text{-}ZnFe_2O_4$) are assumed as magnetic particles. So, before moving to the numerical calculations, it is needed to address some realistic values related to this model. After surveying the studies of Alam et al. and Bongar and Hriczo,[14,41] we found the following thermo-physical values of blood and $Mn\text{-}ZnFe_2O_4$ as shown in Table 1.

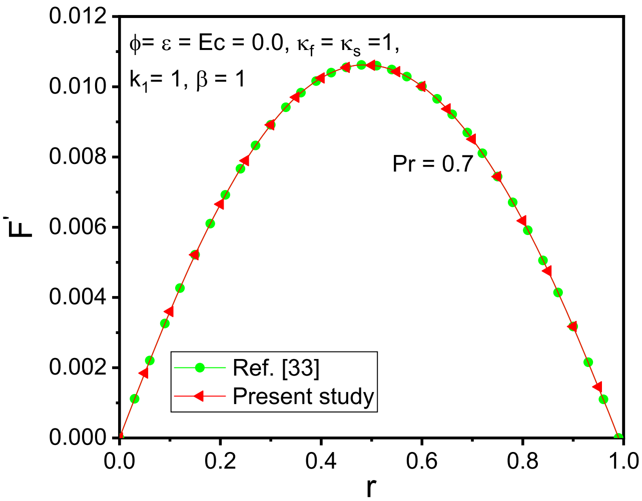

FIGURE 2 Comparison of velocity profile for Prandtl number Pr [Colour figure can be viewed at wileyonlinelibrary.com]

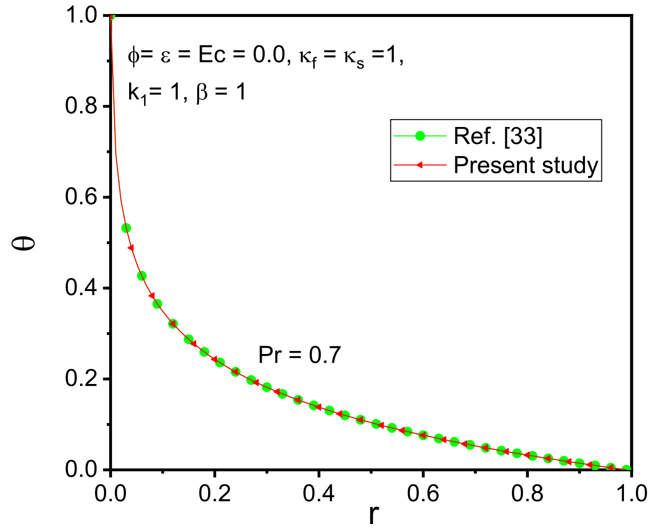

FIGURE 3 Comparison of temperature profile for Prandtl number Pr [Colour figure can be viewed at wileyonlinelibrary.com]

TABLE 1 Thermo-physical values of blood and Mn-ZnFe_2O_4

Physical properties	C_p $(jkg^{-1}K^{-1})$	ρ (kgm^{-3})	κ $(Wm^{-1}K^{-1})$
Blood	3.9×10^3	1050	0.5
$Mn-ZnFe_2O_4$	800	4900	5

Whereas human body temperature is $T_w = 37^0c$,[42] body Curie temperature is $T_c = 41^0c$. Using these values, we found dimensionless Curie temperature $\varepsilon = 78.5$.[8] The values of various parameters that act in this model are Prandtl number $\Pr = 21, 23, 25$,[14] ferromagnetic interaction parameter $\beta = 0, 5, 10, 15$,[8,14] Eckert number $Ec = 0.001, 0.005, 0.1$,[43] volume fraction $\varphi = 0.0, 0.01, 0.03, 0.05, 0.1, 0.2$,[44] and the arbitrary constant $k_1 = -1, -0.5, 0, 1, 5$.[33]

6 | RESULTS AND DISCUSSION

A comprehensive analysis of involving physical parameters is demonstrated graphically and discussed with their respective outcomes throughout Figures 4–9 under representation of dimensionless axial velocity and temperature distributions. The influence of arbitrary constant coefficient, namely, k_1, on velocity and temperature profiles are displayed at Figures 4 and 5. It is clearly seen from these figures that numerical solutions can be obtained by choosing values of negative, positive, or even zero k_1, whereas Abd-el-Malek and Badran[33] found the results only when the values of k_1 are positive. It is observed that the velocity of blood-Mn$ZnFe_2O_4$ reduces with augment values of k_1; whereas the temperature profile is enhanced in this case.

Figures 6 and 7 display the influence of the ferromagnetic interaction parameter on velocity and temperature profiles. As the ferromagnetic number rises, the axial velocity is increased, and the temperature profile is reduced gradually. Noted that, major increment of the blood-Mn$ZnFe_2O_4$ velocity is observed for $\beta = 15$, whereas major reduction of the blood-Mn$ZnFe_2O_4$ temperature is observed for $\beta = 15$. The reason behind that is due to the behavior of polarization/magnetization force on blood that applied perpendicular to the cylindrical surface. The polarization creates a resistance force which is further known as Kelvin force.

The effects of magnetic particles, volume fraction on velocity, and temperature profiles are displayed in Figures 8 and 9, respectively. It can be seen that when the values of magnetic particles volume fraction increase up to 20% in blood, the magnetic fluid velocity decreases, and it's near about $\eta_\infty \approx 0.7$, but after that, the augment of fluid velocity is also noticed. Whereas Figure 9 shows that the fluid temperature increases when the values of φ increase gradually. It is also observed from Figure 9 that blood-Mn$ZnFe_2O_4$ temperature enhancement is much better than pure blood $(\varphi = 0)$.

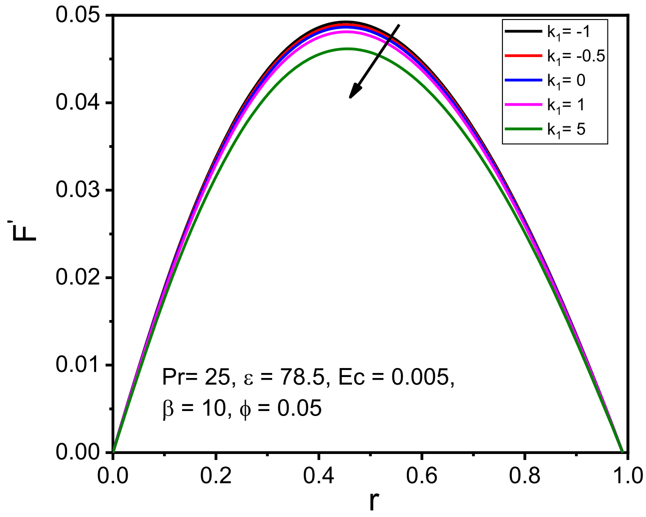

FIGURE 4 Effect of k_1 on velocity profiles [Colour figure can be viewed at wileyonlinelibrary.com]

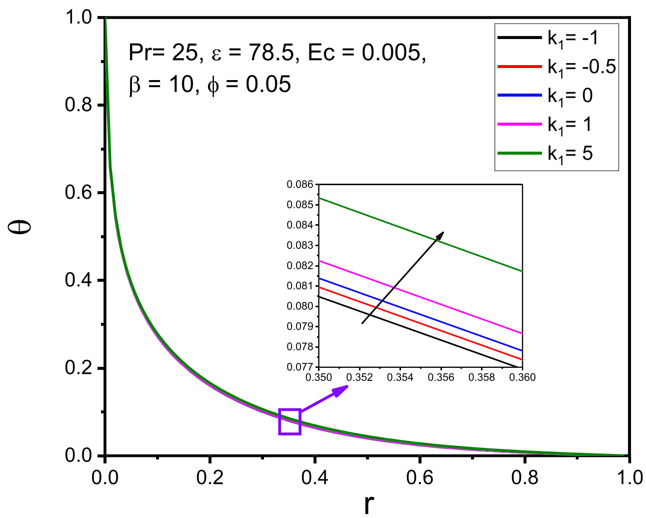

FIGURE 5 Effect of k_1 on temperature profiles [Colour figure can be viewed at wileyonlinelibrary.com]

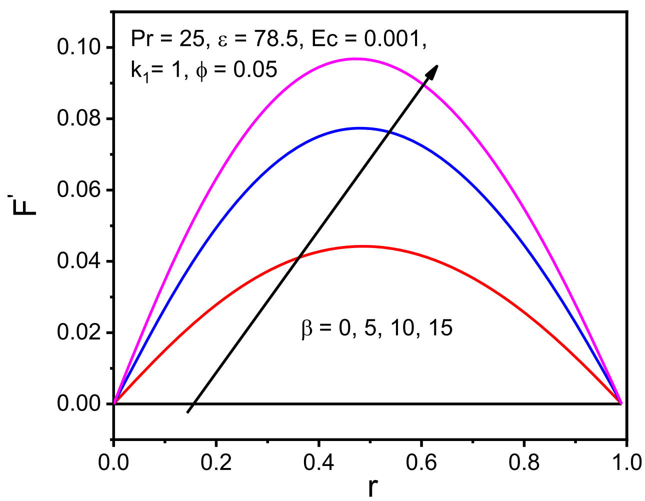

FIGURE 6 Effect of β on velocity profiles [Colour figure can be viewed at wileyonlinelibrary.com]

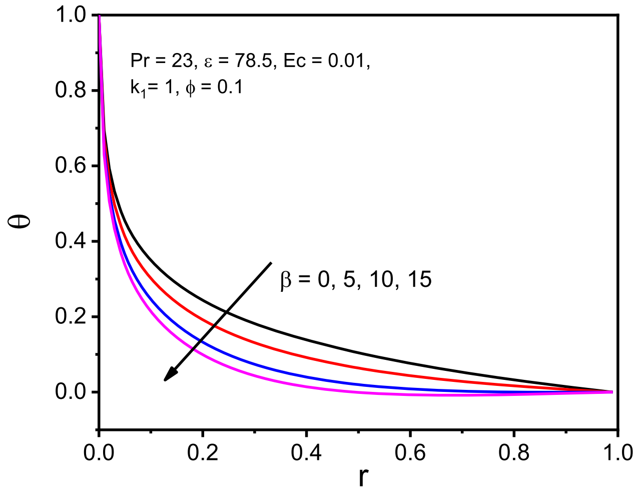

FIGURE 7 Effect of β on temperature profiles [Colour figure can be viewed at wileyonlinelibrary.com]

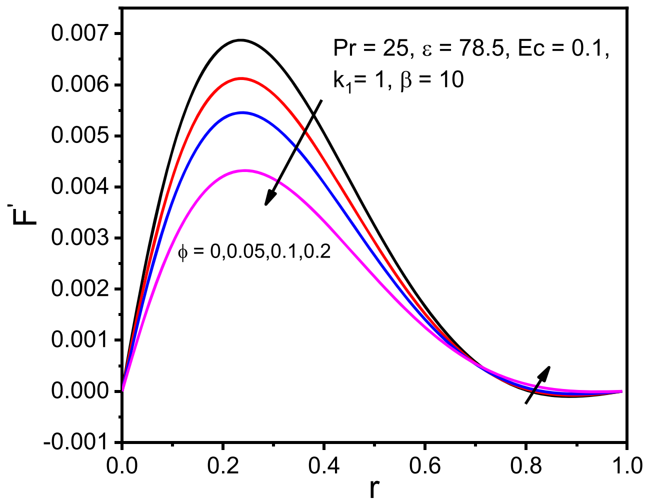

FIGURE 8 Effect of φ on velocity profiles [Colour figure can be viewed at wileyonlinelibrary.com]

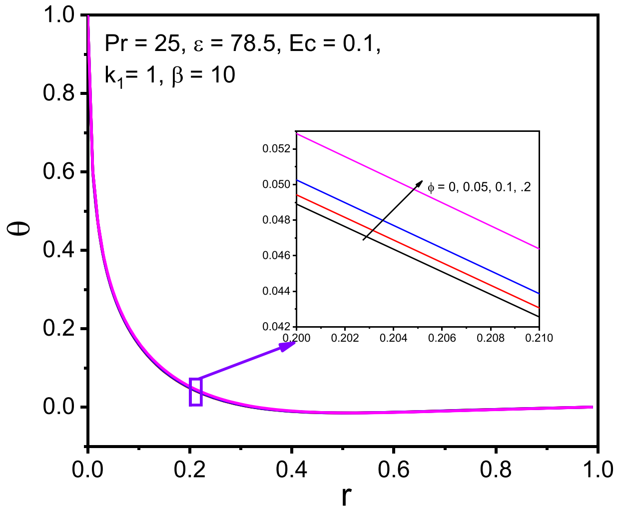

FIGURE 9 Effect of φ on temperature profiles [Colour figure can be viewed at wileyonlinelibrary.com]

The thermal enhancement of base fluid such as blood is found in better position as the better thermal conductivity property of magnetic particles (Mn-ZnFe_2O_4) is applied. This may be also due that magnetic particles spawn friction in blood which creates a resistance to the fluid flow and as a result the fluid velocity reduces.

7 | PHYSICAL QUANTITIES

Another physical interest of this proposed method in engineering point of view is to find out the solutions of skin friction coefficient and the rate of heat transfer. Mathematically, skin friction coefficient C_f and the rate of heat transfer Nu can be defined as,

$$C_f = \frac{2\,\tau_w}{\rho_f\left(\frac{u_0 z^*}{L}\right)^2} \tag{55}$$

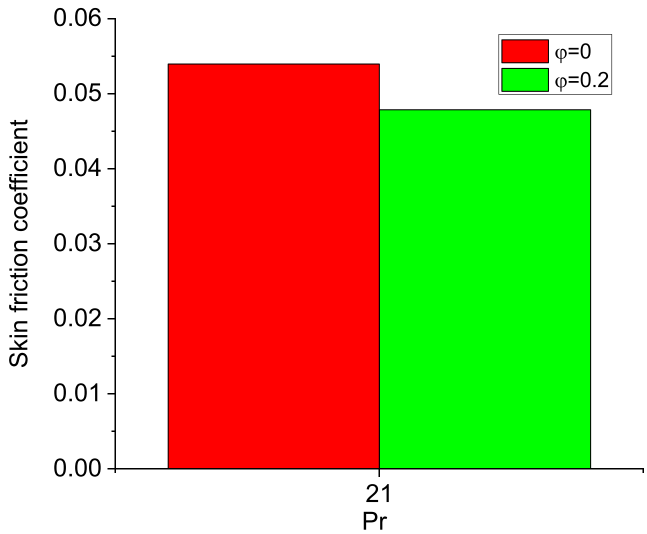

FIGURE 10 Variation of the skin friction coefficient for numerous values of φ [Colour figure can be viewed at wileyonlinelibrary.com]

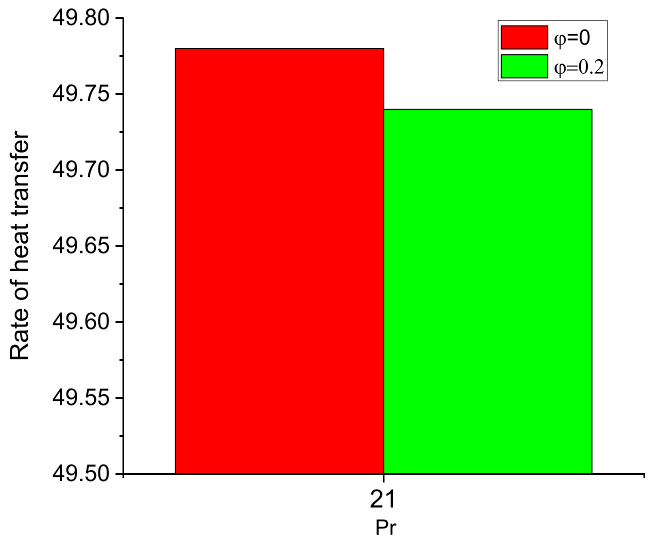

FIGURE 11 Variation of rate of heat transfer for numerous values of φ [Colour figure can be viewed at wileyonlinelibrary.com]

And

$$Nu = \frac{z^* q_w}{\kappa_f (T_c - T_w)} \tag{56}$$

where $\tau_w = \mu_{mf} \left(\frac{\partial u^*}{\partial r^*}\right)_{r^*=R^*}$ and $q_w = \kappa_{mf} \left(\frac{\partial T^*}{\partial r^*}\right)_{r^*=R^*}$. After calculations, we finally get the form of skin friction coefficient and the rate of heat transfer in the following way:

$$C_f = \frac{2\vartheta_f^{\,2}}{(1-\varphi)^{2.5} R^{*4} \left(\frac{u_0 z}{L}\right)^2} \left(\frac{\partial u}{\partial r}\right)_{r=1} \tag{57}$$

And

$$Nu = -\frac{z\kappa_{mf}}{\kappa_f} \left(\frac{\partial \theta}{\partial r}\right)_{r=1} \tag{58}$$

The variation of skin friction coefficient and rate of heat transfer for several values of magnetic particle volume fraction and ferromagnetic number with regard to Prandtl number are displayed in Figures 10–13. These figures show that the skin friction coefficient and rate of heat transfer enhanced monotonically for larger values of ferromagnetic number,

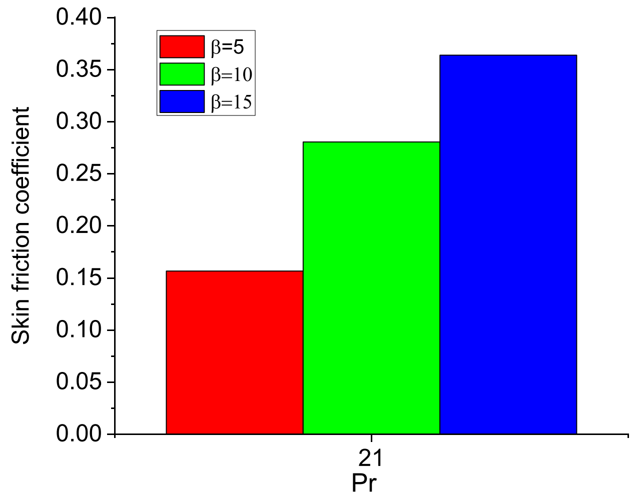

FIGURE 12 Variation of the skin friction coefficient for numerous values of β [Colour figure can be viewed at wileyonlinelibrary.com]

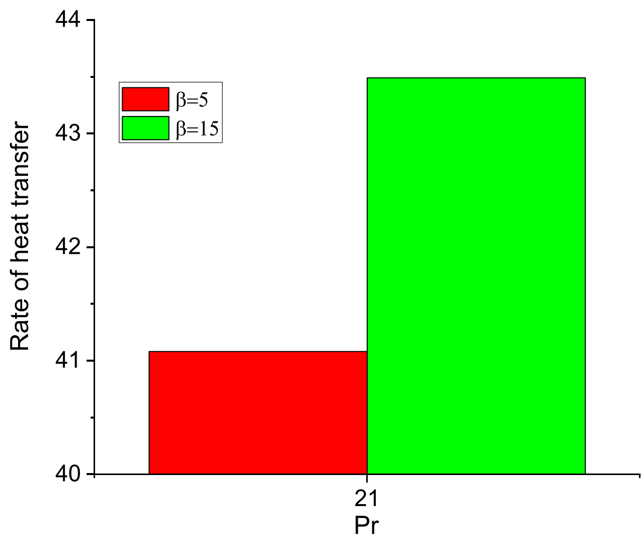

FIGURE 13 Variation of the rate of heat transfer for numerous values of β [Colour figure can be viewed at wileyonlinelibrary.com]

whereas the reverse trend is observed for magnetic particles volume fraction. Physically, this can be explained as that the increment of β leads the Kelvin force as resistance force which has a clear tendency to increase the rate of heat transfer of blood-$MnZnFe_2O_4$ and its augments about 5.86%, whereas the skin friction coefficient is enhanced by 132.22% for $\beta = 5$ to $\beta = 15$. From Figure 12, it also noticed that when the values of φ enhanced from 0 to 0.2, the rate of heat transfer and skin frication coefficient of blood are decreased about 4% and 0.61%, respectively.

8 | CONCLUSIONS

In this work, the flow and heat transfer of biomagnetic fluid with magnetic particles are investigated through a stretched cylinder under the influence of a magnetic dipole, where blood is considered as a base fluid and Mn-$ZnFe_2O_4$ assumed as magnetic particles which are in spherical shape. The governing partial differential equations are solved by applying group theoretical method known as one parameter group method with invariance analysis. By introducing one parameter group method, the set of PDEs is converted into a system of ODEs along with boundary conditions, where the number of independent variables is reduced into one variable. The profiles of velocity, temperature, skin friction coefficient, and rate of heat transfer were numerically calculated and presented graphically by applying an efficient numerical technique that consists of common finite differences method with central differencing, a tridiagonal matrix manipulation, and an iterative procedure. The proposed model can be applied in reducing blood flow during surgeries, drug delivery, and in MRI. Though, from the present investigation, we can draw the following statements:

i. In the presence of magnetic particles, volume fraction and arbitrary constant velocity of blood-Mn-$ZnFe_2O_4$ reduce; whereas reverse trend is observed for ferromagnetic interaction parameter.
ii. For enlarging values of ferromagnetic interaction parameter, the temperature distribution is decreased, whereas the reverse trend is observed for magnetic particles volume fraction and arbitrary constant.
iii. The distributions of velocity, temperature, skin friction coefficient, and rate of heat transfer were numerically obtained for any values of arbitrary constant either positive or negative even zero; whereas Sheikholeslami and Ebrahimpour[24] found the solution only for positive cases.
iv. With increasing values of ferromagnetic number from 5 to 15, the rate of heat transfer augments by 5.86% and skin friction coefficient enhanced by 132.22%.
v. Both the skin friction coefficient and rate of heat transfer reduce as the values of magnetic particles volume fraction are enlarged. Where the rate of heat transfer is reduced about 4% and the skin friction coefficient is about 0.61%.

ACKNOWLEDGEMENT

The authors would like to thank the Ministry of Science and Technology, The People's Republic of Bangladesh for providing the financial support under National Science and Technology (NST) fellowship for this work.

CONFLICT OF INTEREST

This work does not have any conflicts of interest.

AUTHOR CONTRIBUTIONS

Mohammad Ferdows: Project administration, resources, software, supervision. **Jahangir Alam:** Conceptualization, formal analysis, investigation, visualization. **Md. Ghulam Murtaza:** Methodology, validation, visualization. **Efstratios Em. Tzirtzilakis:** Investigation, methodology, supervision.

LIST OF SYMBOLS

(u^*, v^*)	velocity components (m/s)
(z^*, r^*)	components of the cartesian system (m)
R^*	radius of the cylinder (m)
L	characteristic length (m)
u_0	referred velocity (m/s)

H^*,H	magnetic field of strength (A/m)
H_1,H_2	arbitrary function of one-parameter group
$u_w{}^*$	stretched velocity (m/s)
γ	strength of magnetic field at the source position
M	magnetization
K	pyromagnetic coefficient (K^{-1})
Ec	Eckert number
Pr	Prandtl number
k_1,k_2,k_3	arbitrary coefficients
Nu	rate of heat transfer
C_f	skin friction coefficient
ε	dimensionless Curie temperature
β	ferromagnetic interaction parameter
c	distance between the magnetic dipole to sheet (m)
T^*	fluid temperature (K)
T_w	temperature of the sheet (K)
T_c	Curie temperature (K)
C_p	specific heat at constant pressure ($\mathrm{J\ kg^{-1}\ K^{-1}}$)
F'	dimensionless velocity component in z- direction
φ	dimensionless magnetic particles volume fraction
η	dimensionless similarity variable
θ	dimensionless temperature
ψ	stream function
ρ	fluid density ($\mathrm{kg/m^3}$)
μ	dynamic viscosity (kg/ms)
μ_0	magnetic fluid permeability ($\mathrm{NA^{-2}}$)
υ	kinematical viscosity ($\mathrm{m^2/s}$)
ε_1	convergence criteria
κ	thermal conductivity (J/m s K)
ϕ,ω	constant functions

LIST OF ABBREVIATIONS

BFD biomagnetic fluid dynamics
FHD ferrohydrodynamics
MHD magnetohydrodynamics
ODEs ordinary differential equations
PDEs partial differential equations

SUBSCRIPTS AND SUPERSCRIPTS SYMBOLS

$()_{mf}$	magnetic fluid
$()_f$	base fluid
$()_s$	magnetic particles (solid particles)
$()'$	differentiation with respect to η

ORCID

Mohammad Ferdows https://orcid.org/0000-0002-8696-9116

REFERENCES

1. Stark DD, Weissleder R, Elizondo G, et al. Super paramagnetic iron oxide: clinical application as a contrast for MR imaging of the liver. *Radiology*. 1998;168:297-301. doi:10.1148/radiology.168.2.3393649
2. Lu J, Ma S, Sun J, Xia C, Liu C, Wang Z. Magnetese ferrite nanoparticle micellarnanocomposites as MRI contrast agent for liver imaging. *Biomaterials*. 2009;30(15):2919-2928. doi:10.1016/j.biomaterials.2009.02.001

3. Mekheimer Kh S, Abo-Elkhair RE, Abdelsalam SI, Khalid KA, Moawad AMA. Biomedical simulations of nanoparticles drug delivery to blood hemodynamics in diseased organs: Synovitis problem. *Int Commun Heat Mass Transf*. 2022;130:105756. doi:10.1016/j.icheatmasstransfer.2021.105756
4. Durr S, Janko C, Lyer S, et al. Magnetic nanoparticles for cancer therapy. *Nanotechnol Rev*. 2013;2:395-409. doi:10.1515/ntrev-2013-0011
5. Gul A, Tzirtzilakis EE, Makhanov SS. Simulation of targeted magnetic drug delivery: Two-way coupled biomagnetic fluid dynamics approach. *Phys Fluids*. 2022;34:021911. doi:10.1063/5.0080216
6. Haik Y, Chen JC, Pai VM. Development of bio-magnetic fluid dynamics. In: Winoto SH, Chew YT, Wijeysundera NE, eds. *Proceedings of the IX International Symposium on Transport Properties in Thermal Fluids Engineering*. Hawaii, USA: Singapore, Pacific Center of Thermal Fluid Engineering; 1996:121-126.
7. Tzirtzilakis EE. A mathematical model for blood flow in magnetic field. *Phys Fluids*. 2005;17: PMID: 077103-1-14.
8. Murtaza MG, Tzirtzilakis EE, Ferdows M. Effect of electrical conductivity and magnetization on the biomagnetic fluid flow over a stretching sheet. *Z Angew Math Phys*. 2017;68(4):93. doi:10.1007/s00033-017-0839-z
9. Ferdows M, Murtaza MG, Tzirtzilakis EE, Alzahrani F. Numerical study of blood flow and heat transfer through stretching cylinder in the presence of a magnetic dipole. *Z Angew Math Mech*. 2020;100(7):e201900278. doi:10.1002/zamm.201900278
10. Alam MJ, Murtaza MG, Tzirtzilakis EE, Ferdows M. Effect of thermal radiation on biomagnetic fluid flow and heat transfer over an unsteady stretching sheet. *Comput Assist Methods Eng Sci (CAMES)*. 2021;28(2):81-104.
11. Murtaza MG, Ferdows M, Tzirtzilakis EE, Misra JC. Three dimensional biomagnetic Maxwell fluid flow over a stretching surface in presence of heat source/sink. *Int J Biomath*. 2019;12(03):1950036. doi:10.1142/S1793524519500360
12. Choi SUS. Enhancing thermal conductivity of fluids with nanoparticles. In: *Proceedings of the ASME International Mechanical Engineering Congress and Exposition*. San Francisco, CA, USA; 1995:99-105.
13. Gul A, Khan I, Shafie S, Khalid A, Khan A. Heat transfer in MHD mixed convection flow of a ferrofluid along a vertical channel. *PLoS ONE*. 2015;10(11):e0141213. doi:10.1371/journal.Pone.0141213
14. Alam J, Murtaza G, Tzirtzilakis E, Ferdows M. Biomagnetic fluid flow and heat transfer study of blood with gold nanoparticles over a stretching sheet in presence of magnetic dipole. *Fluids*. 2021;6(3):113. doi:10.3390/fluids6030113
15. Gholinia M, Gholinia S, Hosseinzadeh KH, Ganji DD. Investigation on ethylene glycol nanofluid flow over a vertical permeable circular cylinder under the effect of magnetic field. *Results Phys*. 2018;9:1525-1533. doi:10.1016/j.rinp.2018.04.070
16. Saranya S, Al-Mdallal QM. Non-newtonian ferrofluid flow over an unsteady contracting cylinder under the influence of aligned magnetic field. *Case Stud Therm Eng*. 2020;21:100679. doi:10.1016/j.csite.2020.100679
17. Mehmood OU, Bibi S, Jamil DF, Uddin S, Roslan R, Akhir MKM. Concentric ballooned catheterization to the fractional non-Newtonain hybrid nano blood flow through a stenosed aneurysmal artery with heat transfer. *Sci Rep*. 2021;11:20379. doi:10.1038/s41598-021-99499-z
18. Abd Elmabound Y, Mekheimer Kh S, Abdelsalam I. A study of nonlinear variable viscosity in finite tube with peristalsis. *Appl Bionics Biomech*. 2014;11(4):197-206. doi:10.1155/2014/618637
19. Eldesoky IM, Abdelsalam SI, El-Askary WA, Ahmed MM. Concurrent development of thermal energy with magnetic field on a particle-fluid suspension through a porous conduit. *BioNanoScience*. 2017;9(1):186-202. doi:10.1007/s12668-018-0585-5
20. Bhatti MM, Abdelsalam SI. Bio-inspired peristaltic propulsion of hybrid nanaofluid flow with Titanium (Ta) and Gold (Au) nanoparticles under magnetic effects. *Waves Random Complex Media*. 2021;1-26. doi:10.1080/17455030.2021.1998728
21. Thumma T, Mishra SR, Abbas MA, Abdelsalam SI. Three-dimensional nanofluid stirring with non-uniform heat source/sink through an elongated sheet. *Appl Math Comput*. 2022;421:126927. doi:10.1016/j.amc.2022.126927
22. Bhatti MM, Beg OA, Abdelsalam SI. Computational framework of magnetized MgO–Ni/water-based stagnation nanoflow past an elastic stretching surface: application in solar energy coatings. *Nanomaterials*. 2022;12(7):1049. doi:10.3390/nano12071049
23. Sheikholeslami M, Jafaryar M, Gerdoodbar MB. Influence of novel turbulator on efficiency of solar collector system. *Environ Technol Innov*. 2022;26:102383. doi:10.1016/j.eti.2022.102383
24. Sheikholeslami M, Ebrahimpour Z. Thermal improvement of linear Fresnel solar system utilizing Al_2O_3-water nanofluid and multi-way twisted tape. *Int J Therm Sci*. 2022;176:107505. doi:10.1016/j.ijthermalsci.2022.107505
25. Sheikholeslami M, Said Z, Jafaryar M. Hydrothermal analysis for a parabolic solar unit with wavy absorber pipe and nanofluid. *Renew Energy*. 2022;188:9222-9932. doi:10.1016/j.renene.2022.02.086
26. Sheikholeslami M, Ali Farshad S. Nanoparticles transportation with turbulent regime through a solar collector with helical tapes. *Adv Powder Technol*. 2022;33:103510. doi:10.1016/j.apt.2022.103510
27. Birkhoff G. Mathematics for engineers—III: dimensional analysis of partial differential equations. *Electr Eng*. 1948;67(12):1185-1188. doi:10.1109/EE.1948.6444503
28. Birkhoff G. *Hydrodynamics*. Princeton, N.J: Princeton University Press; 1960.
29. Morgan AJA. The reduction by one of the number of independent variables in some systems of nonlinear partial differential equations. *Q J Math*. 1952;3:250-259. doi:10.1093/qmath/3.1.250
30. Michal AD. Differential invariants and invariant partial differential equations under continuous transformation groups in normal linear spaces. *Proc Natl Acad Sci U S a*. 1952;37:623-627.
31. Moran MJ, Gaggioli RA. Similarity analysis of compressible boundary layer flows via group theory. Tech. Summary Report 838, U.S. Army Math Research Center, Madison, WI. 1967.

32. Moran MJ, Gaggioli RA. Reduction of the number of variables is system of partial differential equations with auxiliary conditions. *SIAM J Appl Math*. 1968;16:202-215.
33. Abd-el-Malek MB, Badran NA. Group method analysis of steady free-convective laminar boundary layer flow on a nonisothermal vertical circular cylinder. *J Comput Appl Math*. 1991;36:227-238. doi:10.1016/0377-0427(91)90028-I
34. El-Kabeir SMM, El-Hakiem MA, Rashad AM. Group method analysis for the effect of radiation on MHD coupled heat and mass transfer natural convection flow water vapor over a vertical cone through porous medium. *Int J Appl Math Mech*. 2007;3(2):35-53.
35. El-Kabeir SMM, Gorla RSR, Rashad AM. Unsteady MHD combined convection over a moving vertical sheet in a fluid saturated porous medium with uniform surface heat flux. *Math Comput Model*. 2007;46(3–4):384-397. doi:10.1016/j.mcm.2006.11.010
36. Nadeem S, Ullah N, Khan AU. Akbar T(2017) Effect of homogeneous-heterogeneous reactions on ferrofluid in the presence of magnetic dipole along a stretching cylinder. *Results Phys*. 7:3574-3582. doi:10.1016/j.rinp.2017.09.006
37. Tahir H, Khan U, Din A, Chu YU, Muhammad N. Heat transfer in a ferromagnetic chemically reactive species. *J Thermophys Heat Transf*. 2020;35(2):402-410. doi:10.2514/1.T6143
38. Matuski H, Yamasawa K, Murakami K. Experimental consideration on a new automatic cooling device using temperature sensitive magnetic fluid. *IEEE Trans Magn*. 1997;13(5):1143-1145. doi:10.1109/TMAG.1977.1059679
39. Makinde OD. Stagnation point flow with heat and mass transfer and temporal stability of ferrofluid past a permeable stretching/shrinking sheet. *Defect Diffus Forum*. 2018;387:510-522. doi:10.4028/www.scientific.net/DDF.387.510
40. Kafoussias NG, Williams EW. An improved approximation technique to obtain numerical solution of a class of two point boundary value similarity problems in fluid mechanics. *Int J Numer Methods Fluids*. 1993;17(2):145-162. doi:10.1002/fld.1650170204
41. Bongar G, Hriczo K. Numerical simulation of water based ferrofluid flow along moving surfaces. *Processes*. 2020;8:830.
42. Tzirtzilakis EE, Xenos M, Loukopoulos VC, Kafoussias NG. Turbulent biomagnetic fluid flow in a rectangular channel under the action of a localized magnetic field. *Int J Eng Sci*. 2006;44(18–19):1205-1224. doi:10.1016/j.ijengsci.2006.07.005
43. Ijaz Khan M, Tamoor M, Hayat T, Alsaedi A. MHD boundary layer thermal slip flow by nonlinearly stretching cylinder with suction/blowing and radiation. *Results Phys*. 2017;7:1207-1211. doi:10.1016/j.rinp.2017.03.009
44. Eid MR, Alsaedi A, Muhammad T, Hayat T. Comprehensive analysis of heat transfer of gold-blood nanofluid (Sisko-model) with thermal radiation. *Results Phys*. 2017;7:4388-4393. doi:10.1016/j.rinp.2017.11.004

How to cite this article: Alam J, Murtaza MG, Tzirtzilakis EE, Ferdows M. Group method analysis for blood-Mn-ZnFe_2O_4 flow and heat transfer under ferrohydrodynamics through a stretched cylinder. *Math Meth Appl Sci*. 2022;45(17):11807-11827. doi:10.1002/mma.8482